International Journal of Materials and Chemistry 2017, 7(2): 36-46
DOI: 10.5923/j.ijmc.20170702.03

Temperature Dependent Properties of Spray Deposited Nanostructured ZnO Thin Films

V. P. Deshpande[1,*], S. D. Sartale[2], A. N. Vyas[2], A. U. Ubale[1,*]

[1]Nanostructured Thin Film Materials Laboratory, Department of Physics, Govt. Vidarbha Institute of Science and Humanities, Amravati, India
[2]Thin Film and Nanomaterial Laboratory, Department of Physics, University of Pune, India

Abstract In present investigation, the effect of substrate temperature on structural, optical and electrical properties of spray deposited nanostructured ZnO thin films is studied. XRD studies showed that films are polycrystalline in nature with hexagonal structure. Optical studies revealed the decrease in band gap from 3.31 to 3.23 eV with increase in substrate temperature. The dark electrical resistivity measurement was done by two probe method. It is of the order of 10^{-2} ohm-cm. From TEP measurement it was confirmed that the ZnO films exhibits n-type conductivity. Seebeck's coefficient was also calculated from TEP graph. It is of the order of 8-45 μVK^{-1}.

Keywords Zinc Oxide, Thin films, Chemical spray pyrolysis technique

1. Introduction

In the last decades, research regarding the physical properties of the transparent conducting oxides (TCO) thin films has intensively motivated the research community due to their wide-ranging applications in flat panel display, light emitting diodes and photovoltaic cells [1]. Zinc oxide is one of the important member amongst TCOs. ZnO is commercially available with advantages such as comparatively low cost, environment-friendly non-toxic nature, high resistance to radiation damage, and high thermal and chemical stability. Chemically, ZnO is a simple compound; morphologically, however, this material is very rich in terms of the geometry of its particles. The n-type character of as-grown ZnO has often been attributed to V_O and Zn_i within the ZnO network. It is the deviation from stoichiometry as a result of the presence of the intrinsic native point defects that makes ZnO semiconducting. There are several research groups working all over the world, aiming at the modification of zinc oxide (ZnO) as an alternative to costly ITO [2-4]. Many researchers focused on the investigation of the relationship between the synthesis route of ZnO and its physical properties [5-10]. ZnO particles were largely prepared by using "wet" chemistry or pyrolysis, whereas the vacuum techniques prevailed in making thin ZnO films. The starting zinc compound, chemical composition of solvent, nature of the precipitating agent, pH, temperature, and time of aging influence the size and geometrical shape of ZnO particles [11].

Various methods have been employed for deposition of ZnO based thin films. Such as chemical vapor deposition, thermal evaporation, magnetron sputtering, pulsed laser deposition (PLD), laser chemical vapor deposition, and non-vacuum methods, namely, successive ionic layer absorption and reaction (SILAR), sol-gel spin coating, spray pyrolysis and screen printing [12-20].

The quality and properties of the spray deposited film highly depends on the various process parameters such as spray rate, substrate temperature, nozzle to substrate distance, quantity of spray solution, and precursor concentration. However, the most important parameter is the substrate temperature as it highly affects the film morphology. The higher the substrate temperature, the rougher and more porous are the films. If the temperatures are too low the films are cracked. In between, dense and smooth films can be obtained. The deposition temperature also influences the crystallinity, texture and other physical properties of the deposited films. The present study is focused on the influence of substrate temperature on structural, optical and electrical properties of zinc oxide films deposited by spray pyrolysis technique.

2. Experimental Details

Zinc oxide thin films were deposited by means of chemical spray pyrolysis technique by varying substrate temperatures from 150℃ to 400℃ in the step of 50℃. (Here after the samples deposited at 150℃, 200℃, 250℃, 300℃,

* Corresponding author:
dvarsha07@gmail.com (V. P. Deshpande)
ashokuu@yahoo.com (A. U. Ubale)
Published online at http://journal.sapub.org/ijmc

350℃ and 400℃ are referred as C1, C2, C3, C4, C5 and C6 respectively). Prior to the deposition, the glass substrates were cleaned as discussed in earlier report [21]. For deposition of ZnO films, 0.1M zinc acetate ($(CH3COO)_2$ $Zn.2H_2O$) (AR grade) was prepared with distilled water. Ammonia was used to maintain the pH of solution at 10. The atomization of the solution into a spray of fine droplets was carried out by spray nozzle, with the help of compressed air as carrier gas. During the course of spray, the substrate temperature was monitored using a chromel alumel thermocouple. All the preparative parameters are optimized and discussed earlier [22].

3. Results and Discussion

3.1. XRD Analysis

Figure (1) shows the XRD patterns of ZnO thin films deposited at different temperatures. It reveals that ZnO thin films are nanocrystalline in nature having hexagonal wurtzite structure, which is confirmed from JCPDS card no. 80-0075 [23]. Comparison of standard JCPDS data and observed values is shown in table 1. As reported by several authors [24, 25], our spray deposited ZnO films has preferred orientation along (002). The increase in peak intensity with substrate temperature confirms that crystallinity of ZnO increases with deposition temperature. However, the decrease in the intensity of the peak for sample C6 (ZnO deposited at 400℃) might be due to relatively lower thickness of the film caused by evaporation of primary ingredients before reaching the surface of the substrate.

The grain size of the deposited material was calculated by using Debye Scherrer's formula [26]. The variation of grain size with deposition temperature is shown in figure (2). It is observed that the grain size of ZnO films increases from 70 to 98 nm with substrate temperature from 150 to 350℃ and then again decreases to 94 nm for 400℃. Similar behaviour was observed by Ma et al. [27] in DC sputtered Ga doped ZnO films in the temperature range 150–400℃.

In thin films, strains originate mainly due to a lattice mismatch between the polycrystalline film and the amorphous substrate and/or differences in coefficients of thermal expansion of the film and the substrate. This lattice strain of the film on the substrate can be calculated by using relation,

$$\varepsilon = \frac{\beta Cos\theta}{4} \quad (1)$$

Also dislocation density can be calculated using relation,

$$\delta = \frac{1}{D^2} \quad (2)$$

Where D is the grain size, β is FWHM, and θ is glancing angle. Values of lattice strain and dislocation density are listed in table 2. The total stress in the film commonly consists of two components. One is the intrinsic stress introduced by impurities, defects and lattice distortions in the crystal, and the other is the extrinsic stress introduced by the lattice mismatch and thermal expansion coefficient mismatch between the film and substrate. The strain in the films is likely to be of intrinsic, rather than of thermal origin. The thermal strain introduced by the different linear thermal expansion coefficients of a film ($\alpha_{ZnO} = 4\times10^{-6}\ K^{-1}$) and glass substrate ($\alpha_{glass}=9\times10^{-6}\ K^{-1}$) is significantly smaller than the measured strain. It shows that the measured film stress is mainly caused by the growth process itself. The lattice strain is maximum for film deposited at 150℃, and it decreases as the deposition temperature increases. The decrease in strain at higher substrate temperatures is attributed to annealing effects and consequent reduction in defects [28].

The lattice constants (a = b and c) of the films have been calculated using the equation [26]

$$\frac{1}{d^2} = \frac{4(h^2+\mathrm{hk}+k^2)}{3a^2+(l^2/k^2)} \quad (3)$$

The calculated values of 'a' and 'c' are 3.250 and 5.205 nm respectively. These values are in fair agreement with the standard values taken from the Joint Committee of Powder Diffraction Standards (JCPDS) card no. 80-0075 [23].

3.2. SEM Studies

Figure (3) shows the SEM images of ZnO thin films. All images are homogeneous and have dense surfaces. The increase in grain size with deposition temperature is clearly observed in figure. Initially the grains deposited are spherical in shape. However as the substrate temperature increases, the spherical grains grow further and truned to flakes like structure. However above the optimum substrate temperature 350℃, morphology again turns to the spherical one with smaller grains. It strongly adheres to the substrates and has tightly bounded particles.

The elemental analysis of ZnO film were investigated by EDAX. The EDAX of ZnO films deposited at 200℃ and 350℃ is shown in figure 4(a) and 4(b). Film deposited at higher temperature has more oxygen vacancies / Zn interstitials, which is responsible for decrease in resistivity of film.

3.3. Optical Studies

The optical absorption of ZnO thin films was studied in the wavelength range 350–850 nm and shown in figure (5). The nature of the transition (direct or indirect) was determined by using the relation,

$$\alpha = \frac{A(h\nu-Eg)^n}{h\nu} \quad (4)$$

where, hν is the photon energy, Eg is the band gap energy, A and n are constants. For allowed direct transitions n = 1/2 and for allowed indirect transitions n = 2. The plots of $(\alpha h\nu)^2$ versus hν are shown in figure (6). First of all, from the plot it was determined that the film has direct band gap, and this property is suitable for photovoltaic solar cell applications. Secondly, it was seen from the plot that there is a linear region. The band gap energy of ZnO, Eg was determined by extrapolating this straight line portion to the energy axis for zero adsorption coefficient (α).

The estimated band gap energy of spray deposited ZnO varies from 3.2 to 3.3 eV, which is in good agreement with the values reported by many earlier workers on ZnO thin films [29-31]. Variation in band gap of ZnO films deposited at various temperatures is shown in figure (7).

It is found that the band gap of ZnO films decreases as the deposition temperature increases upto 350℃, and it again rises for higher temperature. This band gap narrowing might be due to the decrease in the transition tail width and shift effect [32, 33], and increased carrier concentration. Also it is well known that the ZnO band gap is particularly very sensitive to small changes in carrier concentration, grain boundary configuration, and film stress [34, 35]. For higher temperature increase in band gap might be due to poor crystallinity of film.

3.4. Photoluminescence Studies

Figure (8) shows the deconvolution of room temperature PL emission spectrum for ZnO sample measured in the wavelength range of 350–650 nm at an excitation wavelength of 330 nm. The ZnO emission is generally classified into two categories. One is the UV emission of the near band edge in the UV region related to free-exciton recombination and the other is the deep-level (DL) emission in the visible range. Especially, the deep-level emission in the ZnO thin films has been attributed to structural defects such as oxygen vacancies and interstitial zinc [36]. In present case, the film shows strong emission at ~389 nm, attributed to near band edge UV luminescence of ZnO [37]. A broad, low intense peak is found around 600 nm i.e. in green yellow region, which is known to arise from oxygen defects and zinc interstitials [38].

Table 1. Comparison of observed crystallographic data of ZnO thin films with standard JCPDS (80-0075) card

Sample	*hkl*	2θ Standard (degrees)	2θ Observed (degrees)	d-values Standard (A^0)	d-values Observed (A^0)
C1	100	31.728	2.81	31.751	2.816
	002	34.440	2.60	34.412	2.604
	101	36.212	2.47	36.182	2.481
	102	47.494	1.97	47.478	1.913
	103	62.80	1.48	62.670	1.480
C2	100	31.728	2.81	31.751	2.816
	002	34.440	2.60	34.412	2.604
	101	36.212	2.47	36.182	2.481
	102	47.494	1.97	47.478	1.913
	103	62.80	1.48	62.670	1.480
C3	100	31.728	2.81	31.760	2.805
	002	34.440	2.60	34.421	2.597
	101	36.212	2.47	36.190	2.476
	102	47.494	1.97	47.490	1.903
	103	62.80	1.48	62.70	1.471
C4	100	31.728	2.81	31.740	2.819
	002	34.440	2.60	34.400	2.609
	101	36.212	2.47	36.176	2.486
	102	47.494	1.97	47.482	1.918
	103	62.80	1.48	62.665	1.486
C5	100	31.728	2.81	31.732	2.820
	002	34.440	2.60	34.420	2.603
	101	36.212	2.47	36.172	2.489
	102	47.494	1.97	47.488	1.921
	103	62.80	1.48	62.660	1.489
C6	100	31.728	2.81	31.75	2.816
	002	34.440	2.60	34.41	2.604
	101	36.212	2.47	36.182	2.481
	102	47.494	1.97	47.478	1.913
	103	62.80	1.48	62.67	1.48

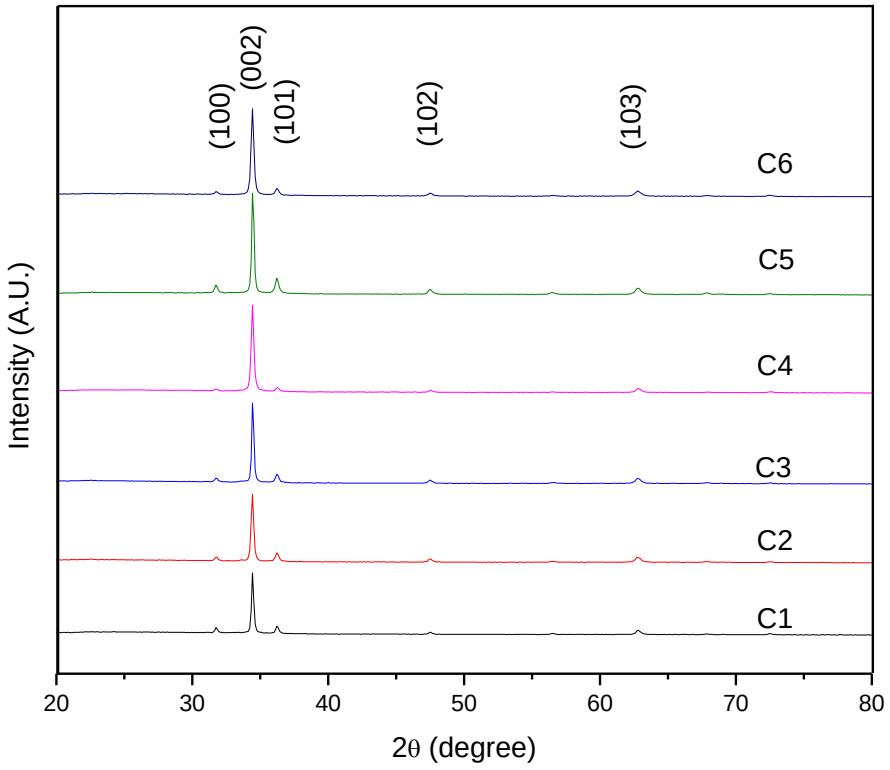

Figure 1. XRD pattern of ZnO thin films deposited at deposited at (C1) 150℃, (C2) 200℃, (C3) 250℃, (C4) 300℃, (C5) 350℃ and (C6) 400℃ temperatures

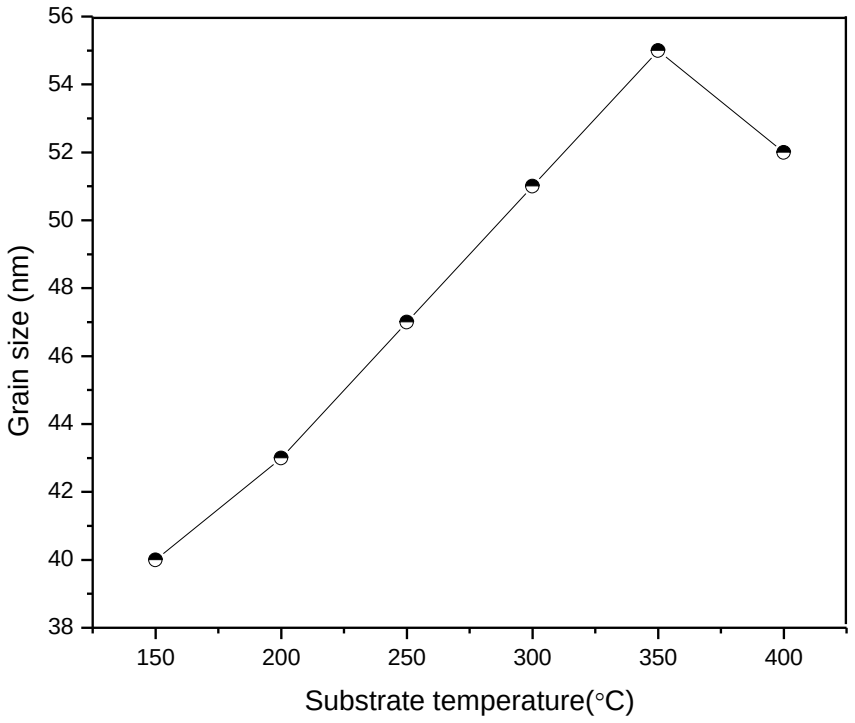

Figure 2. Variation of grain size of ZnO films with substrate temperature

Table 2. Values of grain size, dislocation density, lattice strain, optical band gap, activation energy and Seebeck's coefficient of ZnO thin films

Sample (ZnO deposited at)	Grain size, D (nm)	Dislocation density, 10^{14} lines/m^2	Strain, 10^{-3}	Optical band gap (eV)	Activation energy (eV)	Seebeck's coefficient (μVK^{-1})
C1 (150℃)	40	6.25	0.55	3.31	0.35	8
C2 (200℃)	43	5.40	0.53	3.30	0.30	12
C3 (250℃)	47	4.52	0.50	3.29	0.26	18
C4 (300℃)	51	3.84	0.46	3.28	0.25	25
C5 (350℃)	55	3.30	0.40	3.23	0.22	30
C6 (400℃)	52	3.69	0.42	3.26	0.25	45

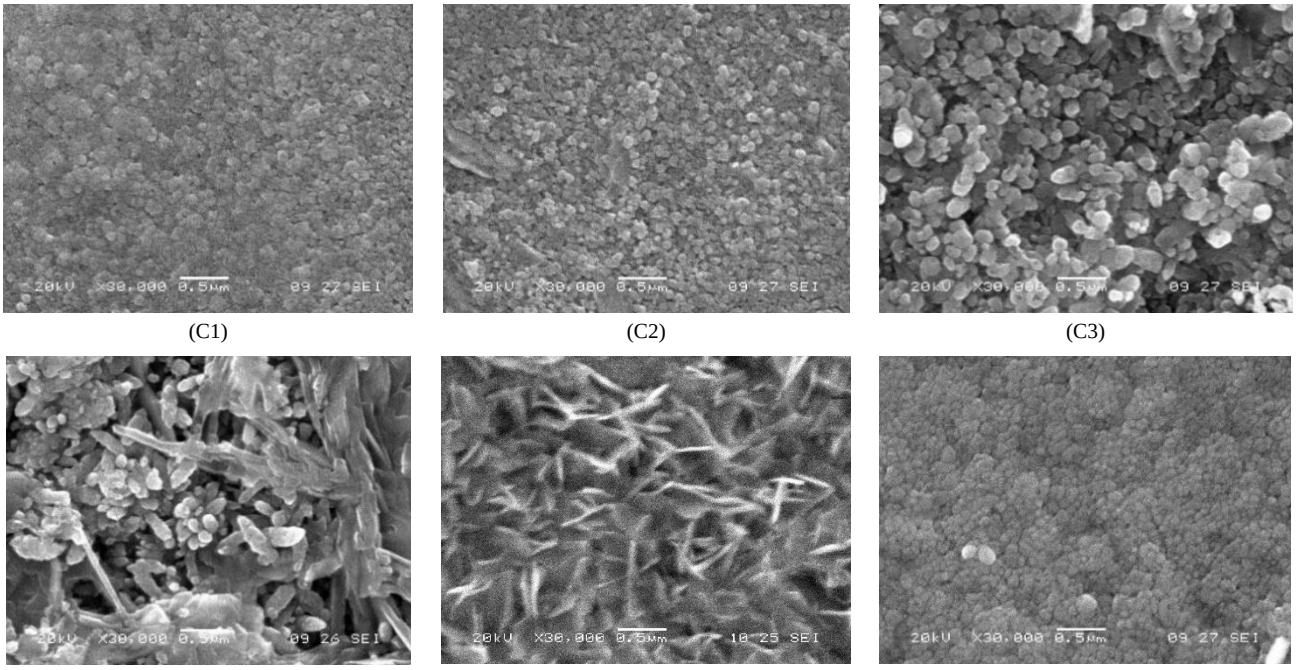

(C1) (C2) (C3)

(C4) (C5) (C6)

Figure 3. SEM of ZnO films deposited at (C1) 150℃, (C2) 200℃, (C3) 250℃, (C4) 300℃, (C5) 350℃ and (C6) 400℃ temperatures

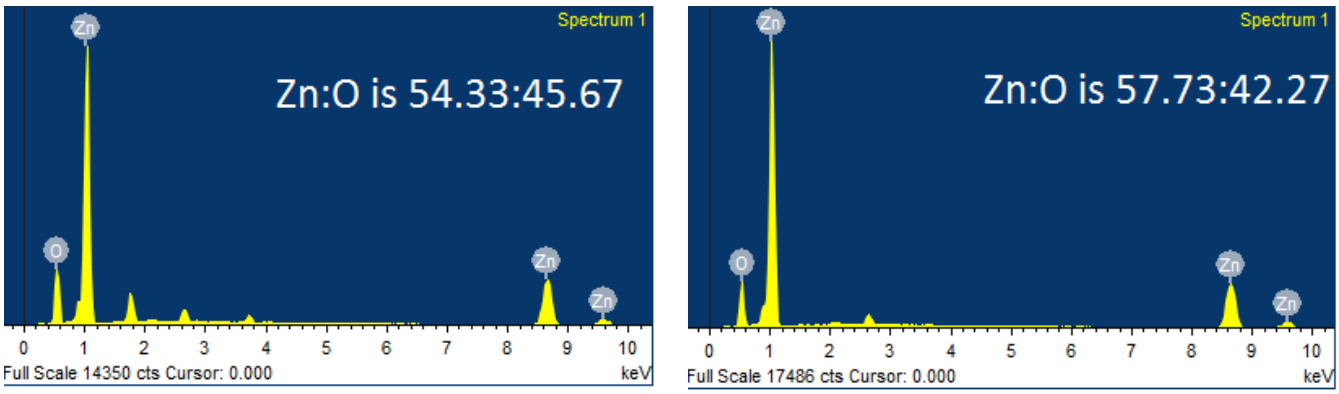

(a) (b)

Figure 4. EDAX spectra of ZnO films deposited at (a) 200℃ and (b) 350℃

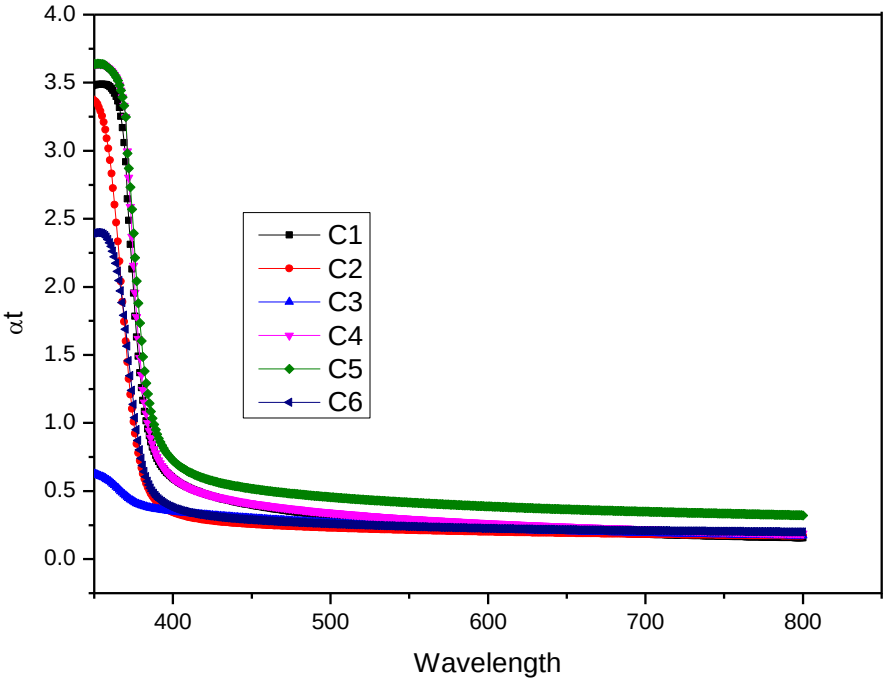

Figure 5. Variation of absorbance of ZnO films deposited at (C1) 150℃, (C2) 200℃, (C3) 250℃, (C4) 300℃, (C5) 350℃ and (C6) 400℃ temperatures

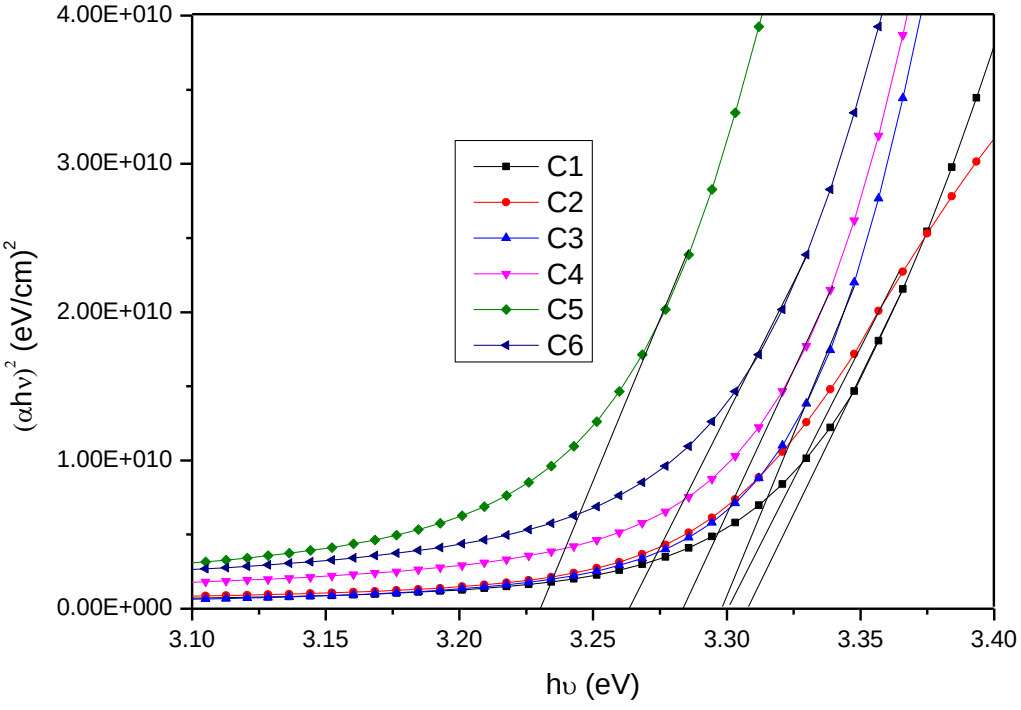

Figure 6. Plot of $(\alpha h\nu)^2$ Vs hν of ZnO films deposited at (C1) 150℃, (C2) 200℃, (C3) 250℃, (C4) 300℃, (C5) 350℃ and (C6) 400℃ temperatures

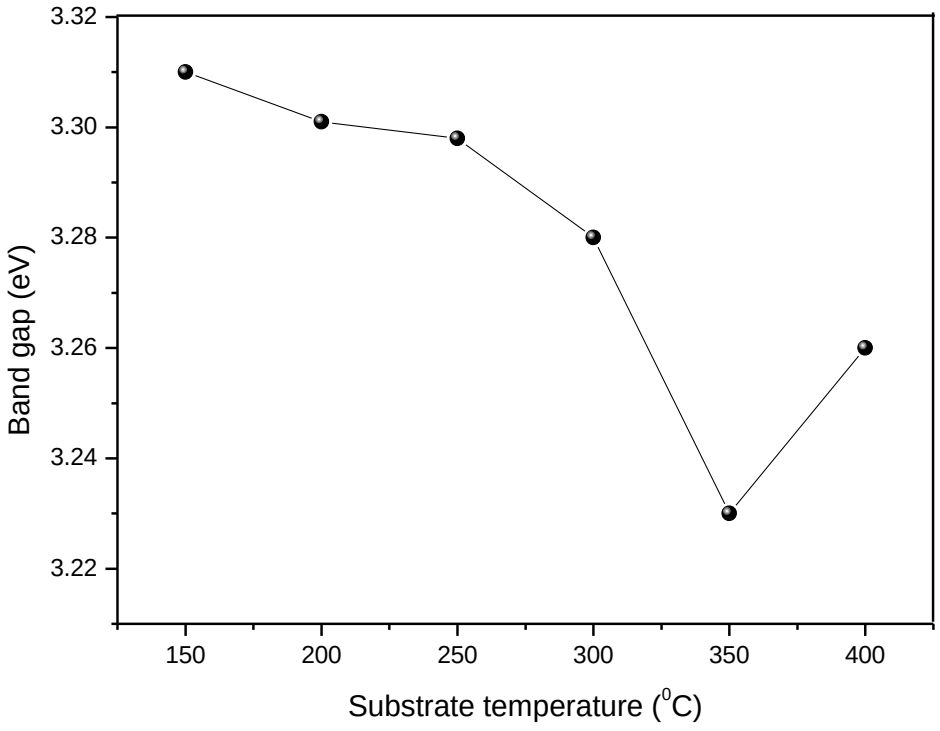

Figure 7. Variation of band gap of ZnO films with substrate temperature

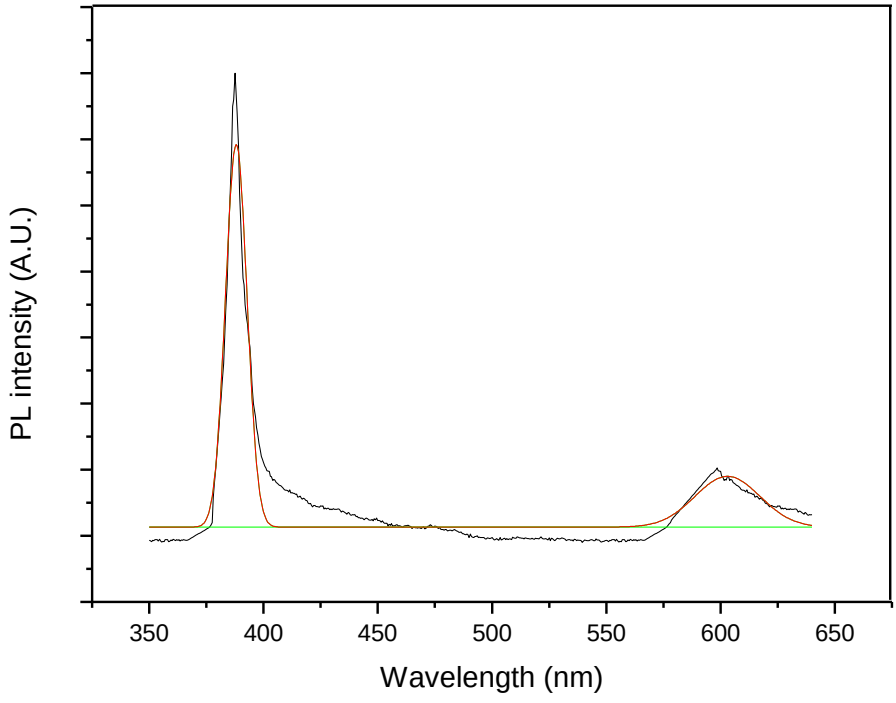

Figure 8. Deconvolution of PL spectra of ZnO thin film deposited at 350℃

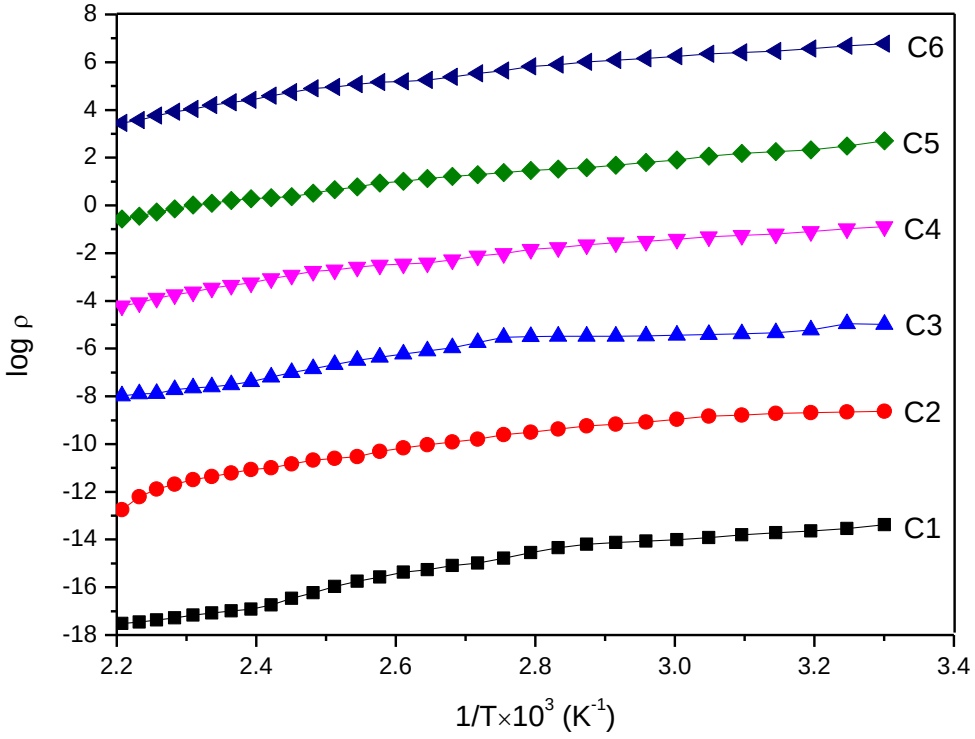

Figure 9. Variation of log ρ Vs $1/T\times10^3$ (K^{-1}) for ZnO thin films deposited at (C1) 150℃, (C2) 200℃, (C3) 250℃, (C4) 300℃, (C5) 350℃ and (C6) 400℃ temperatures

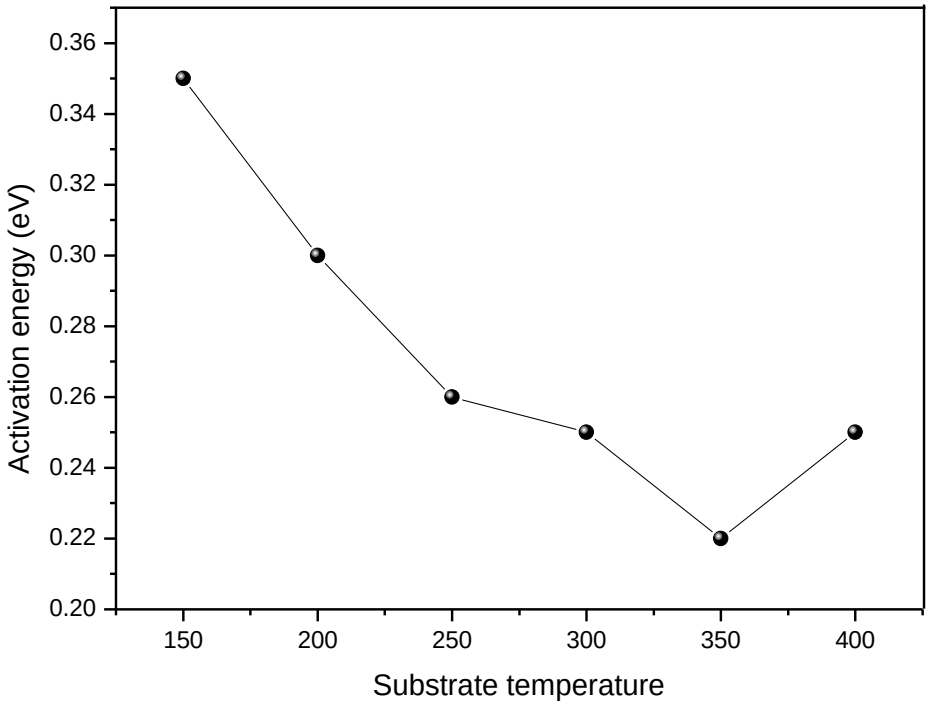

Figure 10. Variation of activation energy of ZnO films with substrate temperature

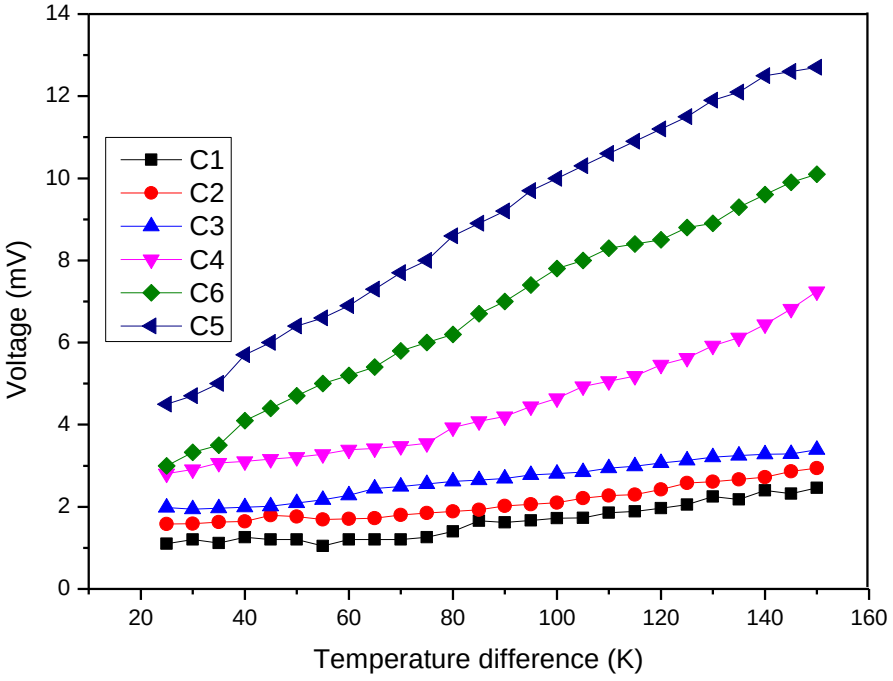

Figure 11. Variation of thermo emf with temperature difference applied across ZnO films deposited at (C1) 150℃, (C2) 200℃, (C3) 250℃, (C4) 300℃, (C5) 350℃ and (C6) 400℃ temperatures

3.5. Electrical Resistivity

Figure (9) shows the variation of the dark electrical resistivity with temperature. It was observed that the resistivity of ZnO thin film decreases with increase in temperature, indicating its semiconducting electrical behaviour. The electrical resistivity is of the order of 10^{-2} to 10^{1} ohm-cm. The films deposited at lower temperature shows higher resistivity than deposited at 350℃. The electrical conduction in ZnO is dominated by electrons generated from O^{2-} vacancies and Zn interstitials. The higher the crystal orientation the lower the resistivity. In fact, this is due to the reduction in the scattering of the carriers at the grain boundaries and crystal defects, which increases the carrier mobility [39, 40].

The thermal activation energy was calculated using the relation,

$$\rho = \rho_0 \exp\left(\frac{Ea}{KT}\right) \quad (5)$$

where, ρ is resistivity at temperature T, ρ_0 is a constant, K is Boltzmann's constant and is Ea the activation energy required for conduction. Variation of activation energy of ZnO thin film with substrate temperature is shown in figure (10). It is found that activation energy is low for the films deposited at 350℃ substrate temperature. The decrease in Ea with increase in substrate temperature may be attributed to change in intercrystalline barrier height caused by the grain size variation.

3.6. Thermo Electric Power Measurement

The temperature gradient applied across the sample causes the transport of carriers from hot to cold end and thus create field which gives thermal voltage. The variation of thermo emf with temperature difference for ZnO films is shown in Figure (11). From thermo emf measurement it was observed that the polarity of thermally generated voltage at the hot end is positive indicating that films are of n-type. The Seebeck's coefficient was determined by calculating the slope of the thermoelectric emf versus the temperature difference between the hot and the cold end of the samples. The value of α i.e. Seeback coefficient is listed in table 2. It is observed that, the Seebeck's coefficient α increases as deposition temperature increases. The relatively high thermoelectric emf of thin films is due to its higher crystallinity and crystallite size.

4. Conclusions

1. In present chapter the effect of substrate temperature on structural, optical and electrical properties of ZnO thin films is studied. For that ZnO thin films were successfully deposited by chemical spray pyrolysis technique in temperature range 150 to 400℃.
2. XRD results showed that ZnO films have pollycrystalline nature with hexagonal wurtzite structure. The grain size of ZnO increases with

substrate temperature. Scanning electron micrograph shows dense structure with spherical grains. At higher temperature this grains grows and exhibits flakes like structure.

3. The observed band gap of ZnO thin films decreases from 3.31 to 3.23 eV with substrate temperature. Photoluminescence study revealed that strong emission at ~389 nm, attributed to near band edge UV luminescence of ZnO.
4. A dark electrical resistivity of ZnO films is calculated by two probe method. It is in the ranged of 10^{-2} to 10^{1} ohm-cm. The activation energy decreases from 0.35 to 0.22 eV nm for substrate temperature 150 to 350℃ and then again increases to 0.25 eV for 400℃. From thermo electric measurement it is observed that the spray deposited ZnO films have n-type conductivity. The Seebeck's coefficient was calculated from the slope of thermo emf graph. Value coefficient α increases from 8 to 45 μV/K with substrate temperature.
5. It is therefore concluded that, the properties of ZnO thin films can be tailored simply by controlling the substrate temperature, which in turn may be employed for a specific application. All the results are summarized in table 2.

ACKNOWLEDGEMENTS

Author is thankful to Deparment of Physics, University of Pune, Pune. The work is partially supported by Departmental Research Development Program of University of Pune, Pune.

REFERENCES

[1] R.G. Jordan, Mater. Res. Bull. 25 (2000) 52.

[2] T. Minami, Mater. Res. Bull. 25 (2000) 38.

[3] T. Minami, H. Nanto and S. Takata, Appl. Phys. Lett. 41 (1982) 958.

[4] T. Minami, H Nanto and S Takata, Japan. J. Appl. Phys.23 (1984) L280.

[5] S. Choopun, R. D. Vispute and W. Noch, Appl. Phys. Lett. 75 (1999) 3947.

[6] Y. Li, G. W. Meng, L. D. Zhang, and F. Phillipp, Appl. Phys. Lett. 76 (2000) 2014.

[7] L. Guo, S. Yang, and C. Yang, Appl. Phys. Lett. 76 (2000) 2901.

[8] R. Wu, C. Xie, H. Xia, J. Hu, and A. Wang, J. Cryst. Growth 217 (2000) 274.

[9] Y. Lia, X. L. Chen, H. Li, M. He and Z. Y. Qiao. J. Cryst. Growth 233 (2001) 5.

[10] B. K. Meyer, H. Alves and D. M. Hofmann Physica Status Solidi B 241 (2004) 231.

[11] S. Music, A. Saric, and S. Popovic, J. Alloys Comp. 448 (2008) 277.

[12] A. K. Das, P. Misra, and L. M. Kukreja, J. Phys. D: Appl. Phys 42 (2009) 165405.

[13] B. Allabergenov, S.-H. Chung, S. M. Jeong, S. Kim, and B. Choi, Opt. Mater. Exp. 31 (2013) 733.

[14] K. P. Misra, R. K. Shukla, A. Srivastava, and A. Srivastava, Appl. Phys. Lett. 95 (2009) 031901.

[15] C. H. Hsu, L. C. Chen, and X. Zhang, Mater. 7 (2014) 1261.

[16] C. Wang, Z. Chen, Y. He, L. Li, and D. Zhang, Appl. Surf. Sci. 255 (2009) 6881.

[17] V. S. Kalyamwar, F. C. Raghuwanshi, N. L. Jadhao, and A. J. Gadewar, J. Sens. Technol. 3 (2013) 31.

[18] F. K. Shan, B. I. Kim and G. X. Liu, J. Appl. Phys. 95 (2004) 4772.

[19] D. Mishra, A. Srivastava, A. Srivastava, and R. K. Shukla, Appl. Surf. Sci. 255 (2008) 2947.

[20] G. Shanmuganathan and I. B. Shameem Banu, Adv. Cond. Matt. Phys. 2014 (2014), Article ID 761960.

[21] A. U. Ubale, V. P. Deshpande, Optoelectron. Adv. Mater. – Rapid Communications Vol. 5(2) (2011) 119.

[22] A.U. Ubale, V.P. Deshpande, J. Alloys Comp. 500 (2010) 138.

[23] Powder Diffraction File, JCPDS-International Center for Diffraction Data, Pennsylvania, 1972.

[24] E.G. Fu, D.M. Zhuang, G. Zhang, Z. Ming, W.F. Yang, J.J. Liu, Microelectron. J. 35 (2004) 383.

[25] F. K. Shan and Y. S. Yu, J. Eur. Ceram. Soc. 24 (2004) 1869.

[26] B.D. Cullity, Elements of X-ray diffraction, Addison-Wesley, New York, 1978.

[27] Q. B. Ma, Z. Z. Ye, H. P. He, J. R. Wang, L. P. Zhu and B. H. Zhao, Vacuum 82 (2007) 9–14.

[28] P. R. Benger, K. Chang, P. Bhattacharya, J. Sing and K. K. Bajaj, Appl. Phys. Lett. 53 (1988) 684.

[29] G. L. Mar, P. Y. Timbrell, and R. N. Lamb, Chem. Mater. 7 (1995) 1890.

[30] Kyu-Seog Hwang, Ju-Hyun Jeong, Young-Sun Jeon, Kyung-Ok Jeon and Byung-Hoon Kim, Ceramics Inter. 33 (2007) 505.

[31] D. Zaouk, Y. Zaatar, R. Asmar and J. Jabbour, J. Microelectron. 37 (2006) 1276.

[32] C. Zhang, J. Phys. and Chem. of Solids 71(2) (2010) 364.

[33] S. Benramache, B. Benhaoua, F. Chabane, and F. Z. Lemadi, J. Semi. 34(2) (2013) 2.

[34] V. Srikant and D. R. Clarke, J. Mater. Res. 12 (1997) 1425.

[35] V. Srikant and D. R. Clarke, J. Appl. Phys. 83 (1998) 5447.

[36] T. Prasada Rao, M. C. Santhosh Kumar, A. Safarulla, V. Ganesan, S. R. Barman and C. Sanjeeviraja, Physica B 405 (2010) 2226.

[37] Y. Ma, G. T. Du, T.P. Yang, D.L. Qiu, X. Zhang, H.J. Yang, Y.T. Zhang, B.J. Zhao, X.T. Yang and D.L. Liu, J. Cryst. Growth 255 (2003) 303.

[38] X.M. Fan, J.S. Lian, Z.X. Guo and H.J. Lu, Appl. Surf. Sci. 239 (2005) 176.

[39] V. Musat, B. Teixeira, E. Fortunato, R.C.C. Monteiro and P. Vilarinho, Surf. Coat. Technol. 180-181 (2004) 659.

[40] Z.Q. Xu, H. Deng, Y. Li, Q.H. Guo and Y.R. Li, Mater. Res. Bull. 41 (2006) 354.